PCCP

Molecular structure and infrared spectra of dimethyl oxalate†

Susy Branco Lopes, Leszek Lapinski and Rui Fausto*

Department of Chemistry, University of Coimbra, 3004-535, Coimbra, Portugal.
E-mail: rfausto@ci.uc.pt

Received 9th August 2001, Accepted 14th December 2001
First published as an Advance Article on the web 4th Feburary 2002

Infrared spectra of dimethyl oxalate isolated in low-temperature argon matrix and of the compound in the solid amorphous and crystalline state are reported. The experimental observations are interpreted in terms of a large amplitude, low frequency vibration along the torsional coordinate O=C–C=O. Assumption of the large amplitude vibration allows consistent explanation of the spectra observed in matrixes and in the gas phase, and the differences between these and the spectrum of the compound in the crystalline state, in which the planar *trans* structure is fixed. IR spectra of crystalline dimethyl oxalate clearly show that in the relaxed crystal lattice only the *trans* form is populated. Davydov splitting, due to the presence of two molecules per unit cell, was observed for several bands in the IR spectrum of the crystalline compound.

Introduction

Dimethyl oxalate (DMO) is the simplest molecule in the series of symmetric diesters. Its structure has been investigated in the past. It is well established that at room temperature, DMO exists as a monoclinic crystal[1] and that molecules of DMO adopt, in the crystalline lattice, the planar *trans* conformation. The comparatively high melting point of DMO (54 °C) may be explained by the stabilization of the crystal by weak intermolecular hydrogen bonds between the hydrogen atoms of methyl groups and the carbonyl groups of the neighbouring molecule.

The infrared spectrum of solid DMO differs significantly from those recorded for the molten compound or DMO in solutions or in the gas phase.[2] This has attracted the attention of spectroscopists. Moreover, the dipole moment of DMO in the centrosymmetric *trans* (C_{2h}) form should be zero, but measurements of this parameter for DMO dissolved in *m*-xylene or dioxane result in values far from zero: 2.0 D and 2.47 D, respectively.[3,4] Different hypotheses have been formulated to explain these observations. In the early works of Saksena[5] and Miyazawa[6] the coexistence of planar *trans* and *cis* forms in the fluid phases was favoured. Wilmshurst and Horwood[2] postulated that a nonplanar C_2 conformation, in which the two groups are rotated by *ca.* 40° (with respect to the planar *trans* structure) around the central C–C bond, is the only form present in the liquid and vapour phases. In such conformation, the lone pair–lone pair repulsion would be avoided. Durig and Brown[7] opted for the *trans* isomer being the only one present in all the phases, with rotation of the methyl groups being the only major structural change between solid and liquid or vapour. In their opinion, no rotation around the carbon–carbon bond was involved in the change of structure of the compound upon conversion from solid to fluid states. Katon and Lin[8] reported some indications of the existence of two isomers (planar *trans* and a second of unknown structure) in fluid states of DMO. In spite of the long lasting discussion, no definitive conclusions about the structure of DMO in the vapour or liquid phase were reached. The hypotheses about the possible structure of the stable conformers of isolated molecules of DMO were based on the registration of broad-contour IR bands of the compound in the vapour or liquid phases. To the best of our knowledge no well-resolved IR spectra of DMO were available in the literature hitherto.

In the present work, we recorded the IR spectra of DMO isolated in noble gas low-temperature matrixes. These resolved spectra, combined with the results of theoretical calculations, allowed us to postulate the structure of isolated molecules of the compound.

Experimental

Commercially available dimethyl oxalate (Aldrich, 99%) was used in this study. Vapours of this compound were deposited together with a large excess of matrix gas (argon 99.9999%, Air Liquide) onto the cold (8 K) CsI mounted on the cold tip of the APD Cryogenics DE-202A closed-cycle helium refrigerator. The concentrations of matrixes were low enough to prevent association of the compound. In order to reduce the vapour pressure over the solid dimethyl oxalate, the glass tube, in which the compound was kept during matrix deposition, was cooled to 258 K. The vapours of the compound were introduced to the cryostat chamber through a micrometer needle valve and the nozzle was kept at room temperature.

A solid amorphous layer was prepared in the same manner as the matrixes but with the flux of matrix gas cut off. The layer was then allowed to anneal at slowly increasing temperature up to 200 K. IR spectra were collected during this process every 20 K. After the temperature exceeded 200 K the substrate was cooled back to 8 K and the final spectrum was recorded.

KBr pellets containing solid DMO were prepared by standard procedures. After the IR spectrum of the pellet at room temperature had been collected, the pellet was heated to a temperature (343 K) above the melting point of DMO and the spectrum was recorded once again.

Infrared spectra of the matrixes were recorded with a resolution of 0.5 cm^{-1} on a Mattson FTIR spectrometer (Infinity 60AR). In the case of solid (amorphous or crystalline) layers the resolution was 1.0 cm^{-1}. The spectra of KBr pellets were recorded with a Bomem MB spectrometer with 4 cm^{-1} resolution. SiC globar sources, KBr or ZnSe beamsplitters and DTGS mid-IR detectors were used in all cases.

† Electronic Supplementary Information available. See http://www.rsc.org/suppdata/cp/b1/b107232n/

 DOI: 10.1039/b107232n

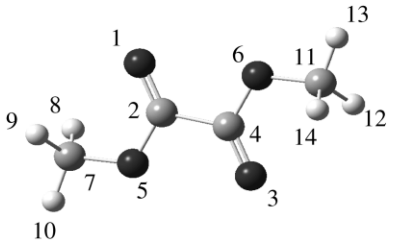

Scheme 1

Computational

The geometries of a series of conformations of DMO were optimized at the DFT(B3LYP)/6-31G++G** and MP2/6-31G++G** levels of theory. For each of the conformations the O=C–C=O torsional angle was fixed (at a value between 0° and 180°) and the remaining parameters were optimized using the partial optimization option (popt = tight) of the Gaussian 98 program.[9] All the optimized geometries were of C_2 symmetry. For the *trans* (180°) and *cis* (0°) conformations the symmetry was higher, C_{2h} and C_{2v}, respectively. At geometries optimized at the DFT(B3LYP)/6-31G++G** level, the harmonic frequencies and infrared intensities were calculated using the same method. For the conformations corresponding to the O=C–C=O torsional angles 140° and 180°, the calculated Cartesian force constants were transformed to the molecule-fixed internal coordinates allowing normal-coordinate analysis to be performed as described by Schachtschneider.[10] The list of symmetry-adapted internal coordinates used in this analysis is given in Table S1 of the ESI;† for the atom numbering see Scheme 1. Potential energy distribution (PED) matrices[11] were calculated and their elements greater than 10% are given in Tables 1 and 2. In order to correct for vibrational anharmonicity, basis set truncation, and the neglected part of electron correlation, the calculated DFT wavenumbers were scaled down by a single factor of 0.978.

Results and discussion

The molecule of DMO consists of two ester groups connected by a single C–C bond. Geometry optimizations carried out for this compound clearly show that in both ester units the –O–Me methoxy fragments adopt the *cis*-ester orientation with respect to the carbonyl C=O group (as shown in Scheme 1), with two out-of-plane hydrogen atoms of a methyl group symmetrically pointing towards the C=O oxygen atom. This corresponds to the usual orientation of methyl groups in methyl carboxylic esters.[12,13,14] *Ab initio* calculated energies of conformers with *trans*-ester orientation of –O–Me groups (with respect to C=O) are higher by more than 30 kJ mol^{-1}. This indicates that those structures are of no practical importance and can be omitted in further discussion.

A theoretical search through the potential energy surface of DMO led to the conclusion that the conformational analysis of the compound can be reduced to consideration of the rotation of the ester units, with respect to each other, around the central C–C bond. Two factors determine the energy of the molecule as a function of this rotation. Firstly, conjugation of the π electron systems of both C=O groups stabilizes the planar geometries. Secondly, lone pair–lone pair repulsion destabilizes the planar conformations, since the overlap of the lone pairs is maximal for these structures.

Theoretical assessment of the energy of the DMO molecule as a function of the rotation around the C–C bond has been undertaken. The O=C–C=O torsion was chosen as the driving internal coordinate. Energies of a series of points were calculated (at the MP2/6-31++G** and DFT(B3LYP)/6-31++G** levels). At each point the O=C–C=O torsion was fixed to a chosen value between 0 and 180° and all other structural parameters were optimized. In a fair approximation the ester groups behaved as rigid units during the optimizations. At each value of the O=C–C=O coordinate the distortions from the C_s local symmetry of the O=C–O–Me units did not exceed 1.5°.

The calculated potential energy profiles are presented in Fig. 1. The balance between the π electron system conjugation and lone pair repulsions makes the theoretical prediction of this energy profile extremely sensitive to the applied theoretical approach. Though in both MP2/6-31++G** and DFT(B3LYP)/6-31++G** calculations the *cis* form (0°) corresponds to a maximum and the energy is minimal in the region of distorted *trans* conformations (close to 140°) , the details of the two curves are not the same. Calculations performed at the DFT level predict a very broad, practically single minimum, centered at 180°, while those undertaken at the MP2 level result in the prediction of a 1.3 kJ mol^{-1} high barrier between the two degenerated by symmetry minima corresponding to the O=C–C=O torsion values of ±135°. However, in both cases, conformations with minimal energy correspond to geometries distorted (with respect to the *trans* C_{2h} form) by 30–40°. On the other hand, it seems that for a theoretical description of a molecule like DMO use of diffusion functions in the basis set is of crucial importance. Indeed, calculations carried out at the MP2/6-31G** and DFT(B3LYP)/6-31G** levels predict both planar forms as minima (sharper for *trans* and shallower for *cis*) with the global minimum at 180° (see Fig. S1 in the ESI†). This is certainly due to the fact that, without diffusion functions in the basis set, the repulsive interactions of the negatively charged oxygen atoms (and their lone pairs) must be underestimated.

The IR spectrum of DMO isolated in an Ar matrix is presented in Fig. 2. The observed bands are listed in Table 1. In a crude approximation this experimental spectrum is fairly well reproduced by the theoretical (DFT) calculation carried out for the *trans* (180°) conformation of the compound. The intense bands at 1762 (νC=O), 1211 (νC–O), 1167 (γCH$_3$)

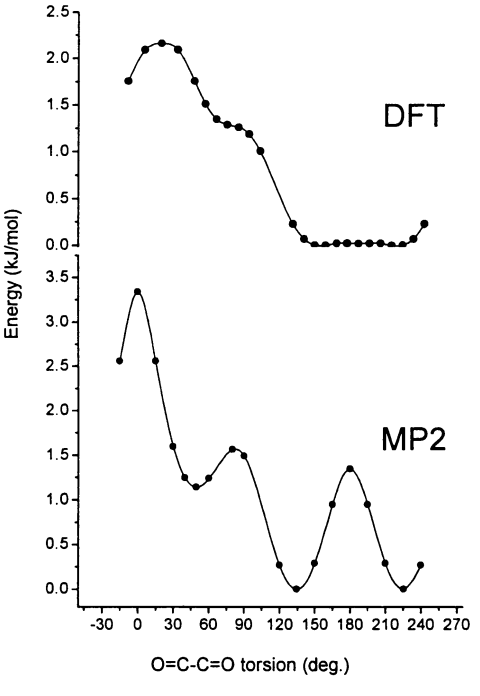

Fig. 1 Electronic energy of DMO calculated (at the DFT(B3LYP)/6-31++G** and the MP2/6-31++G** levels) as a function of O=C–C=O torsion. At each point all remaining geometry parameters were optimized.

Table 1 Frequency and intensities of infrared bands of DMO Isolated in an Ar matrix compared with theoretical DFT (B3LYP)/6-31++G** frequencies (ν), infrared intensities (I) and potential energy distribution (PED) calculated for C_2 conformation corresponding to 140° value of O=C–C=O torsion

ν_{exp}/cm^{-1}	I_{exp}rel.	ν_{calc}[a] /cm^{-1}	I_{calc}/km mol^{-1}	Sym.	PED (%)
3520.2	6				2 × νC=O
		3117	2	A	νCH$_3$asym (97)
3045.6	14	3117	17	B	νCH$_3$asym (98)
3014.7	19	3081	25	A	νCH$_3$asym' (100)
		3081	3	B	νCH$_3$asym' (100)
		2962	0.2	A	νCH$_3$sym (98)
2965.3	39	2962	51	B	νCH$_3$sym (98)
2856.8	8				
2070.4	3				
2027.9	1				
1959.3	4				
1797.8	8				
1789.3	3	1774	59	A	νC=O (87)
1782.5	11				
1769.6	9				
1762.4	469	1764	473	B	νC=O (92)
1756.6	sh				
1727.0	5				
		1465	1	A	δCH$_3$asym (83)
1458.3	21	1465	20	B	δCH$_3$asym (84)
1449.3	17	1456	19	A	δCH$_3$asym' (93)
1444.9	sh				
		1456	1	B	δCH$_3$asym'(93)
		1445	1	A	δCH$_3$sym (84)
1437.4	23	1440	12	B	δCH$_3$sym (92)
1435.4	sh				
1333.1	7				
1322.4	16	1320	33	A	νC–O (46), δCC=O (23), νC–C(20)
1210.5	498	1212	555	B	νC–O (52), γCH$_3$(26)
		1185	0.5	A	γCH$_3$(77), δCH$_3$sym (10)
1166.8	337	1162	210	B	γCH$_3$(55), νC–O (16)
1162.7	sh				
1161.6	sh				
1158.9	sh				
1156.9	sh				
		1146	0.5	B	γCH$_3$'(92)
		1146	2	A	γCH$_3$'(92)
		1011	1	A	νO–CH$_3$ (88)
983.3					
979.3	3				
975.7					
947.4	36	937	32	B	νO–CH$_3$(83), νC–O (13)
		854	1	A	νC–O (28), δCCO (26), νC–C(14)
		824	4	B	γ C=O (93)
775.1	29	762	28	B	δCC=O (30), δCCO (28), δCOC (20)
772.0	sh				
767.3	6				
765.0	sh				
746.5	0.4				
729.2					
727.2	2				
694.3	1				
		630	26	A	γC=O (60),*d* CC=O (19)
		414	9	A	δCC=O (59), νC–C(24), γC=O (21)
		363	3	A	δCOC (29), δCCO (24), νC–C (25)
		328	38	B	δCC=O (50) δCOC (49)
		271	0.05	A	δ COC (53), δCCO (44)
		207	0.5	B	τC–O (59), δCCO (25), δCOC (12)
		143	5	B	δCCO (37), τC–O (27), τCH$_3$(18), δCOC (11)
		130	0.6	A	τCH$_3$(76), τC–O (17)
		122	0.7	B	τCH$_3$(80), τC–O (14)
		108	3	A	τC–O (74), τCH$_3$(23)
		14	5	A	τC–C(103)

[a] Calculated frequencies scaled down by 0.978.

Table 2 Frequencies and intensities of infrared bands of DMO in the crystalline state compared with theoretical DFT (B3LYP)/6-31++G** frequencies (ν) , infrared intensities (I) and potential energy distribution (PED) calculated for the C_{2h} (*trans*) conformer

ν_{exp}/cm^{-1}	I_{exp}rel.	ν_{calc}[a] cm^{-1}	I_{calc}/km mol^{-1}	Sym.	PED(%)
3495	5				
		3116	0	A_g	νCH_3asym (97)
3053	1	3116	20	B_u	νCH_3asym (97)
3024	4	3079	30	A_u	νCH_3asym' (100)
		3079	0	B_u	νCH_3asym' (100)
		3000	0	A_g	νCH_3sym (97)
2968	10	3000	51	B_u	νCH_3sym (97)
2859	2				
2613	2				
2547	2				
2502	1				
2263	1				
2088	2				
1824	3				
		1774	0	A_g	νC=O (86)
1744	630	1767	508	B_u	νC=O (92)
1720					
1687					
		1465	0	A_g	δCH_3asym (83)
1472	7				
1467					
1456	15	1464	21	B_u	δCH_3asym (84)
		1456	0	B_g	δCH_3asym'(93)
1452	15	1456	20	A_u	δCH_3asym' (93)
		1444	0	A_g	δCH_3sym (85)
1438	25	1440	12	B_u	δCH_3sym (92)
1358	10				
1301	1				
1283	2				
		1313	0	A_g	νC–O (47), δCC=O (24), νC–C(19)
1218	401	1216	615	B_u	νC–O (55), γCH_3(22)
		1184	0	A_g	γCH_3(77), δCH_3sym (10)
1181	111	1164	165	B_u	γCH_3(59), νC–O (13)
1170	22				
1161	5				
1159	4				
		1147	0	B_g	γCH_3'(92)
		1147	2	A_u	γCH_3'(92)
		1018	0	A_g	νO–CH_3 (87)
934		938	33	B_u	νO–CH_3 (86), νC–O (14)
927	43				
		854	0	A_g	νC–O (28), δCCO (26), νC–C(14)
		813	0	B_g	γC=O (100)
780		764	28	B_u	δCC=O (30), δCCO (29), δCOC (20)
776	20				
531	44	533	36	A_u	γC=O (93)
525					
		491	0	A_g	δCC=O (71), νC–C(12)
		373	0	A_g	νC–C (40), δCCO (26), δCOC (19)
		337	38	B_u	δCC=O (53), δCOC (48)
		282	0	A_g	δCOC (62), δCCO (38)
		190	0	B_g	τC–O (94)
		161	8	B_u	δCCO (66), δCOC (25)
		132	1	A_u	τCH_3(83), τC–O (13)
		121	0	B_g	τCH_3(92)
		111	3	A_u	τC–O (84), τCH_3(17)
		5	5	A_u	τC–C(104)

[a] Calculated frequencies scaled down by 0.978.

and two bands at lower frequencies 947 (νO–CH_3) and 775 cm^{-1} (δCC=O, δCCO, δCOC) have their obvious counterparts in the theoretical spectrum of the *trans* conformer. However, there are several characteristic features of the experimental spectrum that are not consistent with assumption of the *trans* conformer as the form responsible for the observed spectrum. Weak and structured bands appear at 1798, 1789, 1782, 1770 and 1333, 1322 cm^{-1}, *i.e.* at the positions of the bands with zero intensity in the spectrum of the C_{2h} form. It has been carefully checked that the origin of these bands is not associated DMO. Moreover, counterparts of these bands were previously[2] observed (at 1802, 1793and 1320 cm^{-1}), as much more intense bands, in the spectrum of DMO in the vapour phase. The origin of these extra bands must be a conformation where

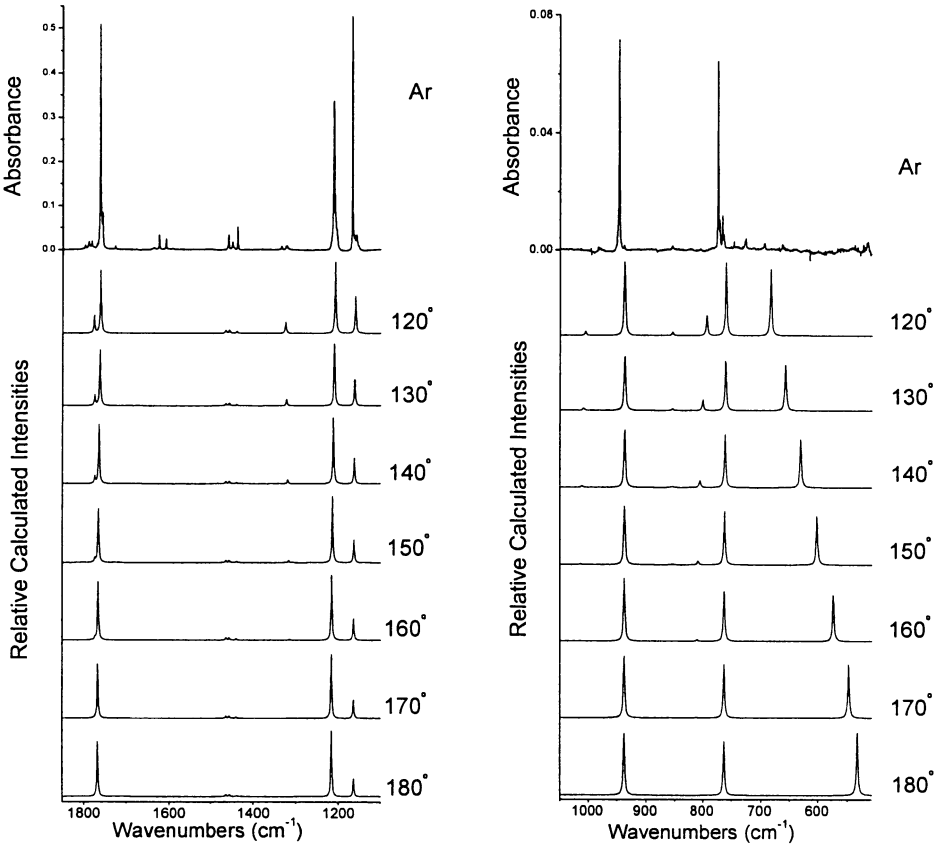

Fig. 2 Infrared spectra of monomeric DMO isolated in an Ar matrix compared with the spectra calculate for a series of values of O=C–C=O tosional angle. Theoretical spectra were calculated at the DFT(B3LYP)/6-31++G** level and scaled down by a factor of 0.978. The bands at 1623.5 and 1607.6 cm^{-1} are due to traces of water.

the O=C–C=O torsional angle is different from 180°. Another observable not consistent with the spectrum predicted for the *trans* isomer is the lack of any significantly strong absorption in the region 700–400 cm^{-1}. Similarly, no absorption was observed in this region in the IR spectrum of the compound in the vapour phase.[2] According to theoretical prediction the intensity of a band around 515 cm^{-1} should be close to the intensities of the bands at 947 and 775 cm^{-1}. In the spectrum of crystalline DMO, where the compound is known to exist as the *trans* conformer, three bands at (933, 926), (780, 776) and (532, 525) cm^{-1} were found (see discussion below) with an intensity pattern matching well the theoretical prediction. This result strongly suggests that the calculated nearly equal intensities of the three bands in question are correct. The appearance of an absorption at a frequency close to 528 cm^{-1} in the crystalline state of DMO and disappearance of this band in fluid phases have been reported previously,[7] but no interpretation of these observations has been proposed. A plausible explanation of these findings can be achieved by considering the effect of the large amplitude vibration associated with the O=C–C=O torsional coordinate on the other molecular vibrations. The profile of the potential energy as a function of the O=C–C=O coordinate is very shallow and the frequency of the vibration along this coordinate is of the order of 10 cm^{-1}. This oscillation is then very slow compared with other higher frequency vibrations. Hence, the more rapid vibrations can be considered as being performed for different, slowly changing geometries of the molecule. A graphical comparison of the experimental spectrum of matrix isolated DMO with the IR spectra calculated for a series of C_2 geometries corresponding to the O=C–C=O torsional angle of 120, 130, 140, 150, 160, 170 and 180° is presented in Fig. 2. The dominant feature in the series of theoretical spectra is the observation that all the strong bands appear in all the spectra at practically the same frequencies. All these bands correspond to vibrations belonging to the B symmetry species (for a C_2 symmetry conformation). The only notable exception is the band at ~520 cm^{-1} (in the spectrum of the *trans* form). This band changes its position considerably as a function of the O=C–C=O angle. If the assumption of a slow, large amplitude vibration along the O=C–C=O torsion is correct, the observed spectrum should be treated as an integral over all the spectra corresponding to different O=C–C=O values (close to the minimum of energy) changing with infinitesimal steps. In such a spectrum, the intensities of the overlapping bands should sum into strong and sharp bands, while the intensity of a band like this at ~520 cm^{-1} should be distributed over a wide range of frequencies and disappear in the background.

In the sequence of spectra calculated for different values of the O=C–C=O angle (Fig. 2), it is clear that with increasing deviation from C_{2h} geometry, the bands, forbidden (because of symmetry) for the *trans* conformation, gain in intensity. Hence, as proposed above, the large amplitude vibration along the O=C–C=O torsional coordinate may be responsible for the appearance of the bands at ~1780 and ~1325 cm^{-1}. Normal modes corresponding to these vibrations are of symmetry A, the same as the low frequency τO=C–C=O vibration, and both the bands appear as if they were modulated by a very low-frequency (close to 10 cm^{-1}) vibration (see Fig. 3). Coupling of the O=C–C=O torsion with the phonons of the matrix may also play a role in this mechanism. Thus, assumption of a large amplitude vibration along the τO=C–C=O coordinate performed by the DMO molecule successfully explains both the observed appearance of the weak and structured bands at ~1780 and ~1325 cm^{-1} and the lack of any significant, sharp absorption feature at wavenumbers close to 520 cm^{-1}.

In the spectrum of DMO in the gas phase[2] the relative intensities of the bands, corresponding to those at ~1780 and

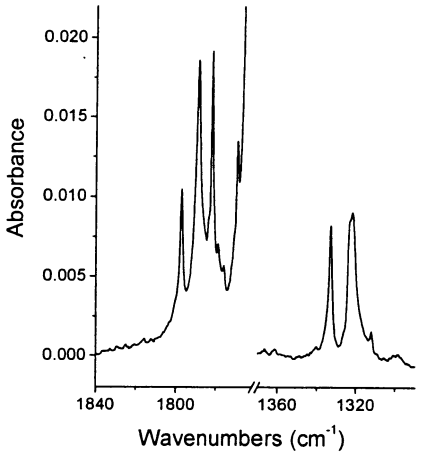

Fig. 3 Two fragments of the infrared spectra of DMO isolated in an Ar matrix.

$\sim$1325 cm^{-1} in the spectra of matrix isolated DMO, are much higher. This can also be explained by considering the influence of the large amplitude τO=C–C=O vibration. Since this torsion has very low frequency (close to 10 cm^{-1}), then, at room temperature, even quite high overtones of this vibration can be significantly populated. This, in turn, would result in an effective higher contribution of geometries corresponding to τO=C–C=O values more distant from 180° to the average molecular conformation. For such geometries, the intensities of the bands forbidden for the *trans* (C_{2h}) conformation become comparable to those allowed for this (C_{2h}) conformation (Fig. S2 in the ESI†). Indeed, in the IR spectrum of gaseous DMO also the other (weaker) bands, predicted to be active only for geometries differing from planar *trans*, become visible.[2]

The appearance of the bands, forbidden by symmetry for the *trans* isomer, could also be explained by assuming the coexistence of well-defined *trans* and (less populated) *cis* isomers of DMO. However, this hypothesis fails to explain the lack of significantly intense IR absorption close to 520 cm^{-1}. This band appears in the spectra predicted for *trans* and *cis* isomers at nearly the same frequency and with nearly the same intensity (compare the predicted spectrum of the *cis* form given in Fig. S2†).

The infrared spectrum of an amorphous, glassy layer of DMO deposited from the vapour phase onto cold (8 K) KBr substrate is presented in Fig. 4A. The "additional" bands (with respect to the spectrum of the *trans* isomer) appear in this spectrum with much higher intensities than in the spectrum of matrix-isolated monomers. According to theoretical predictions these bands should be more intense for conformations of DMO with the O=C–C=O angle more distant from 180°. The observed spectrum corresponds best to that predicted for an O=C–C=O angle close to 90°. For conformations with an O=C–C=O torsional angle lower than 80°, the lower frequency νC=O band (of symmetry B) becomes less intense than the higher frequency νC=O band (A) (Fig. S2†). In an amorphous layer molecules are rapidly frozen from the gas phase without having the possibility of organizing themselves, by forming C–H···O=C bonds, into a regular crystal. The molecules in a glassy layer interact by electrostatic dipole–dipole, dipole-induced dipole and induced dipole-induced dipole forces. These interactions will stabilize conformations with higher values of the dipole moment. The dipole moment of the DMO molecule is a quickly changing function of the O=C–C=O angle (see Fig. 5). Inducing a dipole moment by rotation around the central C–C bond is certainly very easy in a molecule as flexible in this direction as is DMO. Taking into account the accidental orientation of molecules frozen into the amorphous layer one can expect a distribution of different conformations contributing to the observed spectrum. However, the average of the O=C–C=O angle should be close to the perpendicular orientation of both ester units.

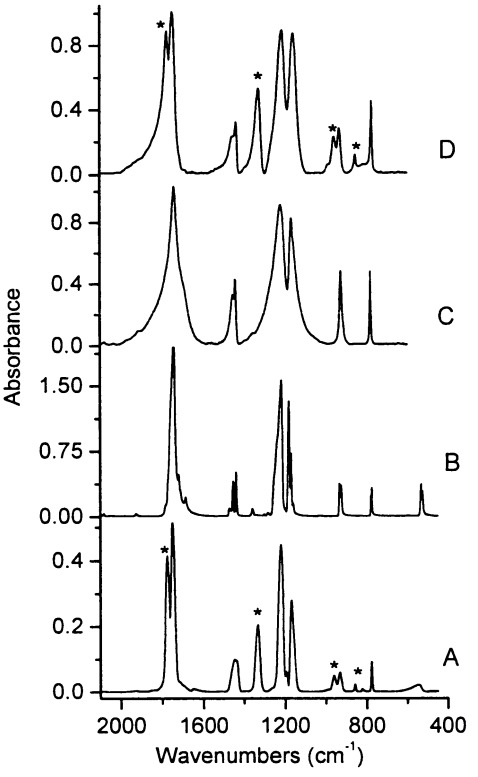

Fig. 4 Infrared spectra of solid DMO: A, amorphous, glassy layer of DMO after deposition at 8 K; B, after annealing to 200 K and cooling to 8 K; C, polycrystalline DMO in KBr pellet at room temperature; D, at 343 K. Bands appearing as a result of breaking of C_{2h} symmetry are marked with asterisks. Note the intensity increase during crystallization of the amorphous layer (traces A and B).

Increasing the temperature of the solid, amorphous layer to 130 K led to the formation of well-organized crystals. The spectrum of the crystalline layer, after annealing to 200 K and cooling back to 8 K is very well reproduced by the theoretically calculated spectrum of the *trans* isomer of DMO, see Fig. 6 and Table 2. It is well known[1] that in the DMO crystal

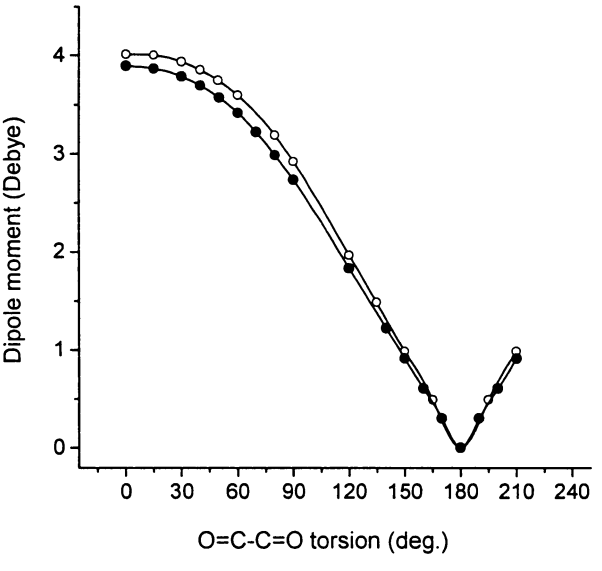

Fig. 5 Dipole moment of DMO molecule calculated at the MP2/6-31++G** (open circles) and DFT(B3LYP)/6-31++G** levels (full circles), as a function of the O=C–C=O torsional angle.

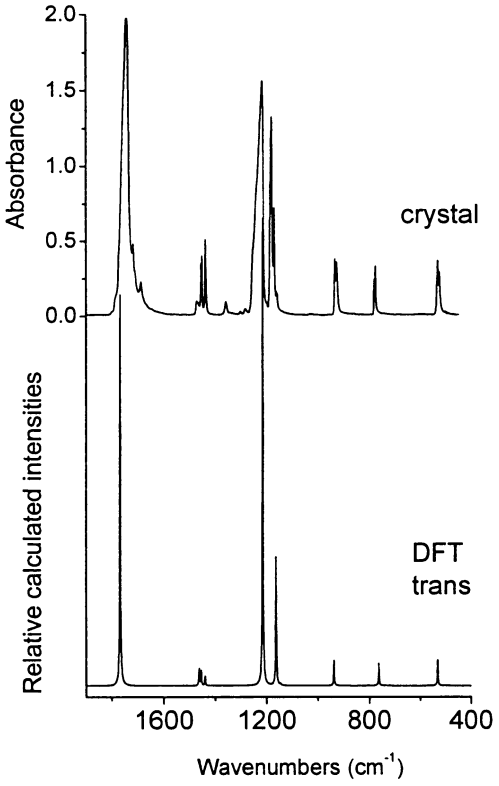

Fig. 6 Comparison of the IR spectrum of DMO crystal obtained by deposition of anamorphous layer at 8 K, annealing to 200 K and cooling to 8 K, with the spectrum theoretically (DFT(B3LYP)/6-31G**) predicted for the *trans* isomer.

all the molecules adopt the *trans* form and that the compound crystallizes in the monoclinic space group, with two molecules per unit cell. Crystals of DMO, prepared by the method described above, must have a very regular structure. This was revealed by the observation of the factor-group (Davydov) splitting of the bands at 933, 926 cm^{-1}, 780, 776 cm^{-1} and 532, 525 cm^{-1}, in the lower frequency range (see Fig. 7). The two observed components of these bands are separated by 7, 4 and 7 cm^{-1}, respectively. The magnitude of the Davydov splitting for DMO was previously predicted[15, 16] as being of the order of 5 cm^{-1}, but the splitting itself is now experimentally observed for the first time.

The infrared spectrum of polycrystalline DMO pressed into a KBr pellet is similar to that of the well-organized crystal (Fig. 4B and C), though, as expected, in the case of the polycrystalline sample the bands are broader. After warming the pellet above the melting point of the compound (to 343 K), new bands appeared in the IR spectrum (Fig. 4D). These bands nicely correspond to those observed in the spectra of the amorphous layer. In neat liquid,[2] as well as for DMO in solutions, the dipole-induced dipole interactions will favour conformations with higher value of dipole moment and lower value of O=C–C=O torsional angle. As in the case of the amorphous layer, the spectra of structures with O=C–C=O angle close to 90° correspond well to the spectra of molten DMO.

Conclusion

Interpretation of the IR spectra of dimethyl oxalate (isolated in low temperature matrixes and in solid amorphous layers) in terms of a large amplitude vibration performed by the molecule along the O=C–C=O torsional coordinate leads to a consistent explanation of the observed spectral features. The assignment of the IR spectra of isolated DMO molecules has been performed. For DMO in the crystalline state, Davydov splitting was observed for several IR bands.

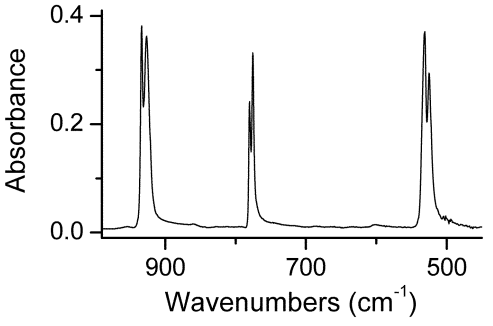

Fig. 7 Factor-group (Davydov) splitting of the IR bands in the spectrum of DMO crystal prepared by deposition of an amorphous layer at 8 K, annealing to 200 K and cooling to 8 K.

Acknowledgement

The authors are obliged to the referees of this paper for their helpful comments.

The financial support of the Portuguese Foundation for Science and Technology (Research Project PRAXIS/P/QUI/10137/1998) is acknowledged.

References

1 M. W. Dougill and G. A. Jeffrey, *Acta Crystallogr.*, 1953, **6**, 831.
2 J. K. Wilmshurst and J. F. Horwood, *J. Mol. Spectrosc.*, 1966, **21**, 48.
3 A. Aihara and M. Davies, *J. Colloid Sci.*, 1956, **11**, 671.
4 R. J. W. LeFevre and A. Sudaram, *J. Chem. Soc.*, 1962, 3904.
5 B. D. Saksena, *Proc. Indian Acad. Sci. Sect. A*, 1940, **12**, 416.
6 T. Miyazawa, *J. Chem. Soc. Jpn.*, 1954, **75**, 540.
7 J. R. Durig and S. C. Brown, *J. Mol. Struct.*, 1976, **31**, 11.
8 J. E. Katon and S. -L. Lin, *J. Mol. Struct.*, 1978, **48**, 335.
9 M. J. Frisch, G. W. Trucks, H. B. Schlegel, G. E. Scuseria, M. A. Robb, J. R. Cheeseman, V. G. Zakrzewski, J. A. Montgomery, Jr., R. E. Stratmann, J. C. Burant, S. Dapprich, J. M. Millam, A. D. Daniels, K. N. Kudin, M. C. Strain, O. Farkas, J. Tomasi, V. Barone, M. Cossi, R. Cammi, B. Mennucci, C. Pomelli, C. Adamo, S. Clifford, J. Ochterski, G. A. Petersson, P. Y. Ayala, Q. Cui, K. Morokuma, D. K. Malick, A. D. Rabuck, K. Raghavachari, J. B. Foresman, J. Cioslowski, J. V. Ortiz, A. G. Baboul, B. B. Stefanov, G. Liu, A. Liashenko, P. Piskorz, I. Komaromi, R. Gomperts, R. L. Martin, D. J. Fox, T. Keith, M. A. Al-Laham, C. Y. Peng, A. Nanayakkara, M. Challacombe, P. M. W. Gill, B. Johnson, W. Chen, M. W. Wong, J. L. Andres, C. Gonzalez, M. Head-Gordon, E. S. Replogle and J. A. Pople, *Gaussian 98, Revision A.9*, Gaussian, Inc., Pittsburgh, PA, 1998.
10 J. H. Schachtschneider, Technical Report; Shell Development Co., Emeryville, CA, 1969.
11 G. Keresztury and G. Jalsovszky, *J. Mol. Struct.*, 1971, **10**, 304.
12 R. Meyer, W. Caminati and H. Hollenstein, *J. Mol. Spectrosc.*, 1989, **137**, 87.
13 R. Fausto and J. J. C. Teixeira-Dias, *J. Mol. Struct. (Theochem)*, 1987, **150**, 381.
14 A. Kulbida and R. Fausto, *J. Chem. Soc., Faraday Trans.*, 1993, **89**, 425.
15 J. F. Landry, C. P. Nash and D .S. Tinti, *J. Mol. Spectrosc.*, 1976, **60**, 1.
16 G. N. R. Tripathi and J. E. Katon, *Chem. Phys.*, 1980, **45**, 141.